0013-7227/08/$15.00/0
Printed in U.S.A.

Endocrinology 149(4):1581–1590

doi: 10.1210/en.2007-1148

Adipose-Specific Disruption of Signal Transducer and Activator of Transcription 3 Increases Body Weight and Adiposity

Erin R. Cernkovich, Jianbei Deng, Michael C. Bond, Terry P. Combs, and Joyce B. Harp

Department of Nutrition, University of North Carolina at Chapel Hill, Chapel Hill, North Carolina 27599

To determine the role of STAT3 in adipose tissue, we used Cre-*loxP* DNA recombination to create mice with an adipocyte-specific disruption of the STAT3 gene (ASKO mice). aP2-Cre-driven disappearance of STAT3 expression occurred on d 6 of adipogenesis, a time point when preadipocytes have already undergone conversion to adipocytes. Thus, this knockout model examined the role of STAT3 in mature but not differentiating adipocytes. Beginning at 9 wk of age, ASKO mice weighed more than their littermate controls and had increased adipose tissue mass, associated with adipocyte hypertrophy, but not adipocyte hyperplasia, hyperphagia, or reduced energy expenditure. Leptin-induced, but not isoproterenol-induced, lipolysis was impaired in ASKO adipocytes, which may partially explain the increased cell size. Despite reduced adiponectin and increased liver triacylglycerol, ASKO mice displayed normal glucose tolerance. Overall, these findings demonstrate that adipocyte STAT3 regulates body weight homeostasis in part through direct effects of leptin on adipocytes. (*Endocrinology* 149: 1581–1590, 2008)

OBESITY IS A significant medical and public health concern due to its prevalence, associated comorbidities, and economic impact (1). At the cellular level, obesity is characterized by an increase in adipose tissue mass, which occurs when adipocytes increase in size through the storage of excess energy as triacylglycerol (TAG) and/or when adipocytes increase in number through the conversion of preadipocytes to adipocytes (2).

The process of fat cell formation or adipogenesis is triggered by extracellular factors that mediate a series of coordinated intracellular events culminating in the expression and activation of several transcription factors. Members of the CCAAT/enhancer-binding protein (C/EBP) and peroxisome proliferator-activated receptor (PPAR) families are well known to regulate these processes (3). Recent studies have implicated members of the signal transducer and activator of transcription (STAT) family of transcription factors in adipogenesis as well (4, 5). STAT3, for example, is abundantly expressed in preadipocytes and adipocytes (4) and highly activated and bound to DNA in proliferating preadipocytes and adipocytes (5). In addition, inhibition of endogenous STAT3 expression with antisense morpholino oligonucleotides significantly decreases preadipocyte proliferation (5). Although changes in expression and activation of STAT3 occur throughout adipogenesis, the precise role of this transcription factor in preadipocyte proliferation and conversion to adipocytes is not yet known.

The weight-reducing effects of the STAT3-activating ligands leptin, IL-6, and ciliary neurotrophic factor (CNTF) also implicate STAT3 in the regulation of adipocyte size. These cytokines have been shown to regulate fat cell size via direct peripheral effects on adipocytes. Leptin regulates fat cell size peripherally by stimulating white adipose tissue (WAT) lipolysis, inhibiting lipogenesis, and promoting fatty acid oxidation (6–13). IL-6 also stimulates WAT lipolysis and has been shown to cause a notable decline in the uptake of circulating TAG by decreasing lipoprotein lipase activity (14–18). Similarly, CNTF inhibits WAT fatty acid biosynthesis via repression of fatty acid synthase (FAS) and sterol regulatory element-binding protein-1 (SREBP-1) gene expression (19, 20). It is thought that the antilipogenic and prolipolytic actions of leptin, IL-6, and CNTF may account for a portion of the weight-reducing effects of these cytokines. Because STAT3 is a downstream target of leptin, IL-6, and CNTF signaling, STAT3 likely mediates many of the effects of these cytokines in adipocytes. The contribution of STAT3 to these aspects of body weight homeostasis, however, has yet to be determined.

To determine the role of STAT3 in adipogenesis and body weight homeostasis, we generated mice with an adipocyte-specific disruption of the STAT3 gene using aP2-Cre-*loxP* DNA recombination. The late deletion of STAT3 induced by the aP2 promoter and the resulting preservation of STAT3 expression in preadipocytes prevented us from examining the role of STAT3 in adipogenesis. Therefore, this report examines the role of STAT3 in mature adipocytes. Here we reveal that adipocyte STAT3 is essential for body weight homeostasis, and its deficiency causes higher body weight and increased adiposity. Furthermore, ASKO mice have reduced serum adiponectin levels and increased liver lipid

First Published Online December 20, 2007

Abbreviations: BAT, Brown adipose tissue; CNTF, ciliary neurotrophic factor; CoA, coenzyme A; ES, embryonic stem; FAS, fatty acid synthase; FFA, free fatty acid; HZ, heterozygous; rLeptin, recombinant leptin; STAT, signal transducer and activator of transcription; TAG, triacylglyceride; VO_2, oxygen consumption; WAT, white adipose tissue; WT, wild type.

***Endocrinology* is published monthly by The Endocrine Society (http://www.endo-society.org), the foremost professional society serving the endocrine community.**

deposits but do not develop impaired glucose tolerance or other obesity-related metabolic perturbations. Thus, ASKO mice represent a model of obesity dissociated from impaired glucose tolerance, and their characterization provides insight into the physiological roles of STAT3 in adipocyte metabolism.

Materials and Methods

Construction of the STAT3 targeting vector

A STAT3 targeting vector was constructed that introduced *loxP* sites upstream and downstream of exon 22. The OSfrt-*loxP* plasmid (kindly provided by the Animal Models Core at the University of North Carolina at Chapel Hill) served as the backbone for the STAT3 targeting vector. STAT3 homologous sequences were amplified and cloned into the OSfrt-*loxP* plasmid containing the neomycin resistance (*neo*) gene, the herpes simplex virus thymidine kinase gene, FRT sites flanking *neo* to facilitate removal of *neo* by FlpE recombinase, a *loxP* site to facilitate removal of the targeted exon by Cre recombinase, and five unique restriction sites. The long arm of homology, spanning exon 21 of the STAT3 gene, was amplified from 129/SvEv genomic DNA. PCR amplification introduced a *Spe*I restriction site and an *Age*I restriction site at the 5′ end and 3′ end, respectively. The resulting 3.3-kb PCR product was *Spe*I/*Age*I digested and cloned into a *Spe*I/*Age*I-digested OSfrt-*loxP* plasmid. The short arm of homology, spanning exons 23 and 24 of the STAT3 gene, was amplified from 129/SvEv genomic DNA. PCR amplification introduced a *Bam*HI restriction site and a *Sal*I restriction site at the 5′ end and 3′ end, respectively. The resulting 2.4-kb PCR product was *Bam*HI/*Sal*I digested and cloned into a *Bam*HI/*Sal*I-digested OSfrt-*loxP* plasmid containing the long arm. The target arm, spanning exon 22 of the STAT3 gene and including a tyrosine residue necessary for STAT3 activation, was amplified from 129/SvEv genomic DNA. PCR amplification introduced a *loxP* site upstream of exon 22 and an *Age*I restriction site and a *Xho*I restriction at the 5′ end and 3′ end, respectively. The resulting 339-bp PCR product was *Age*I/*Xho*I digested and cloned into an *Age*I/*Xho*I-digested OSfrt-*loxP* plasmid containing the long arm and short arm.

Generation of STAT3$^{flox/+}$ mice

A total of 2×10^7 129/SvEv embryonic stem (ES) cells was transfected with 20.0 μg of the linearized STAT3 targeting vector by electroporation (250 μF/300 V). Cells were subjected to selection with G418 and gancyclovir. Surviving colonies were picked after 12–14 d of selection and screened for homologous recombination by PCR and Southern blot analysis. ES cell clones carrying the desired homologous recombination event were expanded. To remove *neo*, expanded clones were electroporated with a vector that transiently expresses FlpE recombinase (kindly provided by the Animal Models Core at the University of North Carolina at Chapel Hill). Deletion of the selection cassette was confirmed by PCR and Southern blot analysis. Targeted clones not containing *neo* were microinjected into blastocysts derived from C57BL/6 females. To generate mice chimeric from the targeted ES cells and host blastocysts (STAT3$^{flox/+}$), microinjected blastocysts were transferred to the uterus of pseudopregnant C57BL/6 recipients. Chimeric mice (as determined by coat color) were then bred with C57BL/6 mice to transmit the targeted allele through the mouse germline. The presence of the targeted allele in the agouti-colored offspring was confirmed by PCR.

Generation of adipose tissue-specific STAT3 knockout mice

Agouti mice heterozygous (HZ) for the targeted STAT3 gene (STAT3$^{flox/+}$) were crossed with transgenic mice expressing Cre recombinase under the control of the adipocyte-specific aP2 promoter/enhancer [B6.Cg-Tg (Fabp4-cre) 1Rev/J; Jackson Laboratories, Bar Harbor ME]. Offspring inheriting both the targeted allele and the Cre-expressing transgene (aP2-Cre STAT3$^{flox/+}$) were intercrossed to yield six derivative strains: 1) STAT3$^{+/+}$ [wild-type (WT)], 2) STAT3$^{flox/+}$ (WT), 3) STAT3$^{flox/flox}$ (WT), 4) STAT3$^{+/+}$/Cre (WT), 5) STAT3$^{flox/+}$/Cre (HZ), and 6) STAT3$^{flox/flox}$/Cre (ASKO). ASKO mice and WT and HZ littermate controls maintained on a mixed background were studied for further analysis.

Animals and PCR genotyping

ASKO mice and littermate controls were housed two to five per cage in a temperature- and humidity-controlled pathogen-free facility, exposed to a 12-h light, 12-h dark cycle, and fed a standard Purina rodent chow (LabDiet ProLab Isopro RMH 3000; PMI Nutrition International, St. Louis, MO) and water *ad libitum*. All protocols for animal use and euthanasia were reviewed and approved by the University of North Carolina at Chapel Hill Institutional Animal Care and Use Committee.

Genotyping was performed by PCR amplification of genomic DNA isolated from tail tips of 3- to 4-wk-old mice. The primers for identifying a floxed allele (5′-GCAAGACTGG ATGGCAAACCGCTATAACTT-3′ and 5′-TCG GCAGGTCAATGGTATTGCTGCAGGTCG-3′) amplify a 682-bp fragment. The primers for identifying a WT allele (5′-AGGAATAGG GAGGACATGGGGTGAGAGTTACCGTG-3′ and 5′-TCGGCAGGTCAATGGTATTGCTGC AGGTCG-3′) amplify a 262-bp fragment. The primers for identifying the Cre transgene (5′-GCGGTCTGGCAGTAAAAACTATC-3′ and 5′-GTGAAACAGCATTGCTGTCACTT-3′) amplify a 100-bp fragment. To detect Cre-mediated recombination, primers were designed that are located on the *loxP* site (5′-GCAAGACTGGATGGCAAACCGCTATAACTT-3′) and exon 23 (5′-TCGGCAGGTCAATG GTATTGCTGCAGGTCG-3′). This primer pair gives rise to a 682-bp fragment or a 336-bp PCR fragment before and after Cre-mediated recombination, respectively. In all cases, PCR was performed using the GeneAmpPCR Fast PCR Master Mix (Applied Biosystems, Foster City, CA). PCR conditions were 94 C for 2 min followed by 35 cycles of 94 C for 1 sec and 64 C for 20 sec. A final extension step of 1 min at 72 C was performed to ensure complete synthesis of all annealed products.

Primary preadipocyte isolation and culture

WAT was aseptically removed from male mice, and stromal vascular cell cultures were established as previously described (21). Briefly, WAT was excised from freshly killed ASKO mice and littermate controls. After excision, adipose tissue was minced into small pieces, washed in DMEM supplemented with 1% BSA, and centrifuged at $1000 \times g$ for 10 min to remove blood cells. Tissue was then decanted into DMEM containing 1.0 mg/ml type I collagenase and digested for 45 min at 37 C with constant end-over-end inversion. After the digestion, adipose cells and stromal vascular cells were separated by centrifugation at $500 \times g$ for 10 min. The stromal vascular cell pellet was resuspended and cultured in DMEM containing 10% vol/vol fetal bovine serum, 10 mg/ml streptomycin, 100 U/ml penicillin, and 1 mM pyruvate at 37 C in 5% CO_2 air. To induce differentiation, 2-d postconfluent preadipocytes were treated with Zen-Bio (Raleigh, NC) differentiation medium. On d 3, the differentiation medium was replaced with Zen-Bio adipocyte maintenance medium, which was changed every 2 d thereafter until analysis on d 8.

For analysis of lipolysis, on d 8, primary cells were incubated in the presence of vehicle, 1.0 μM isoproterenol, or recombinant leptin (R&D Systems, Minneapolis, MN), in doses ranging from 5.0–100.0 ng/ml. After 24 h of incubation, glycerol released into the medium was measured using the Zen-Bio adipocyte lipolysis assay kit.

Immunoblot analysis

Primary cells were washed twice in PBS with 1 mM orthovanadate and then placed immediately in sample buffer [1% Nonidet P-40, 20 mM Tris-HCl (pH 8.0), 150 mM NaCl, 1 mM EDTA, 0.1% NaN_3, 10 μg/ml aprotinin, 1 μM pepstatin, 16.4 μg/ml leupeptin, 1 mM phenylmethylsulfonyl fluoride, 0.1 mM Na_3VO_4, 2% SDS, 10% glycerol]. Tissues were homogenized in sample buffer with a PRO Scientific PRO 200 homogenizer (Oxford, CT). Primary cell lysates, and heart, liver, kidney, hypothalamus, WAT, and brown adipose tissue (BAT) homogenates were heated, and protein concentrations were determined using Bio-Rad Laboratories, Inc. (Richmond, CA) DC protein determination kit. BSA was used as a standard. Samples were heated for 2 min at 85 C, separated by 10% SDS-PAGE, and analyzed by immunoblotting. Immunoblots were developed with the Pierce (Rockford, IL) enhanced chemiluminescence kit.

Dual-energy x-ray absorptiometry measurement of body composition

Body composition was determined on anesthetized male mice using the Lunar PIXImus densitometer (GE Lunar Corp., Madison, WI).

Indirect calorimetry

Oxygen consumption (VO_2), activity (horizontal, vertical, and ambulating), and food intake were measured using an Oxymax open-circuit indirect calorimetry system (Columbus Instruments International, Columbus, OH). Male mice were placed in calorimeter chambers for 5 d in a light- (12-h light. 12-h dark cycle) and temperature-controlled environment. Mice were maintained with free access to standard Purina rodent chow and water throughout the duration of the 5-d measurement period. On d 5, lean mass was measured using the Lunar PIXImus densitometer. Oxygen consumption and activity data are reported as the mean VO_2 and mean counts, respectively, of d 2–4. Food intake data are reported as the mean daily intake of d 1–5.

Biochemical assays

Blood was collected from cut tail tips of conscious male mice in either the fed or the fasting state. Glucose was measured by the glucose oxidase method with a commercial glucometer (FreeStyle Flash blood glucose monitoring system). Blood was also obtained via retroorbital sinus of anesthetized male mice in either the fed or the fasting state. Plasma was collected in EDTA-coated capillary tubes and separated via centrifugation at 3000 × *g* for 10 min. Plasma was used for measurement of insulin. Serum was collected in plain capillary tubes, allowed to clot at room temperature for 20 min, and then separated via centrifugation at 3000 × *g* for 10 min. Serum was used for measurement of leptin, adiponectin, TAG, and free fatty acids (FFAs). Plasma insulin and serum leptin levels were measured by ELISA (Crystal Chem, Downers Grove, IL). Serum adiponectin levels were measured by ELISA (R&D Systems). Serum TAG was measured by colorimetric enzyme assay (Stanbio, Boerne, TX), and FFA levels were in serum were measured using the NEFA-kit-C (Wako Chemicals GmbH, Neuss, Germany). Metabolic parameters measured in the fed state were in animals with free access to food and assayed at 2300 h; for fasted-state measurements, mice were assayed at 0800 h after a 24-h fast in a clean cage free of bedding.

Glucose tolerance test

Oral glucose tolerance tests were performed on male mice that did not have access to food for 4 h before administration of 2.5 mg/g body weight glucose load by oral gavage. Glucose measurements were taken before oral gavage and 15, 30, 45, 60, 90, 120, and 150 min after oral gavage. To measure corresponding insulin levels, plasma was collected from cut tail tips before oral gavage and 15 and 30 min after oral gavage.

Tissue TAG

The tissue lipid extraction procedure was adapted from methods previously described (22).

Histology

Tissues from male mice were fixed in 10% phosphate-buffered paraformaldehyde, embedded in paraffin, and sectioned (5.0 μm) for hematoxylin/eosin staining.

Statistical analysis

All values are expressed as means ± SE. An unpaired Student's *t* test was used to assess statistical differences between ASKO mice and WT or HZ littermate controls. A *t* test with a P value < 0.05 was considered statistically significant.

Results

Generation of STAT3$^{flox/+}$ mice

To determine the role of STAT3 in adipogenesis and body weight homeostasis, we generated mice with an adipocyte-specific disruption of the STAT3 gene using aP2-Cre-*loxP* DNA recombination. We constructed a STAT3 targeting vector with *loxP* sites flanking exon 22 of the murine STAT3 gene (Fig. 1A). Deletion of the *loxP*-flanked exon 22 by Cre recombinase was predicted to produce a truncated nonfunctional translational product missing a tyrosine residue (Tyr 705) essential for STAT3 activation (23).

The STAT3 targeting vector was linearized and electroporated into 129/SvEv ES cells (Fig. 1B). Gancyclovir- and G418-resistant clones were screened for homologous recombination by PCR and Southern blot analysis. Correctly targeted clones were transiently transfected with FlpE recombinase to delete *neo* (Fig. 1C). Deletion of the selection cassette was confirmed by PCR and Southern blot analysis. Targeted ES cell clones devoid of *neo* were microinjected into C57BL/6 blastocysts, and mice carrying the floxed STAT3 allele (STAT3$^{flox/+}$) were created as described in *Materials and Methods*.

Creation of ASKO mice

ASKO mice were generated by breeding mice heterozygous for the targeted STAT3 gene (STAT3$^{flox/+}$) and transgenic mice expressing Cre recombinase under the control of the adipocyte-specific aP2 promoter/enhancer as described in *Materials and Methods* (Fig. 1D). ASKO mice were obtained at the expected Mendelian frequency and exhibited normal growth until the age of 9 wk.

STAT3 expression was examined in tissue lysates from control and ASKO mice by Western blot analysis using an anti-STAT3 antibody that recognizes the C-terminal portion of the STAT3 protein. STAT3 expression was preserved in the heart, liver, kidney, and hypothalamus of ASKO mice (Fig. 1E). By contrast, STAT3 expression was significantly reduced in WAT and BAT from ASKO mice (Fig. 1E). The remaining STAT3 expression was likely derived from stromal vascular cells that did not express aP2. STAT3 expression was not altered, however, in either WAT or BAT obtained from WT or aP2-Cre STAT3$^{flox/+}$ (HZ) mice, suggesting that neither the *loxP* modification nor expression of the aP2 transgene altered the expression of STAT3. These mice were considered controls.

The marked increase in aP2 expression during adipogenesis and the abundance of aP2 mRNA and protein in mature adipocytes established aP2 as a late marker of adipocyte differentiation (24). aP2 is also expressed in preadipocytes (25) and was recently identified as a marker for committed human preadipocytes (26). To define the timing of Cre-mediated STAT3 deletion in ASKO mice, preadipocytes isolated from WT, HZ, and ASKO were differentiated in culture, and lysates were recovered 0, 2, 4, 6, and 8 d after stimulation with differentiation medium. Western blot analysis revealed disappearance of STAT3 expression beginning on d 6 of adipogenesis (Fig. 1F). STAT3 expression in preadipocytes, however, was preserved, suggesting that the Cre transgene was sufficient to direct recombination only in mature adipocytes. Therefore, ASKO mice and WT and HZ littermate controls were studied to establish the role of STAT3 in mature adipocytes.

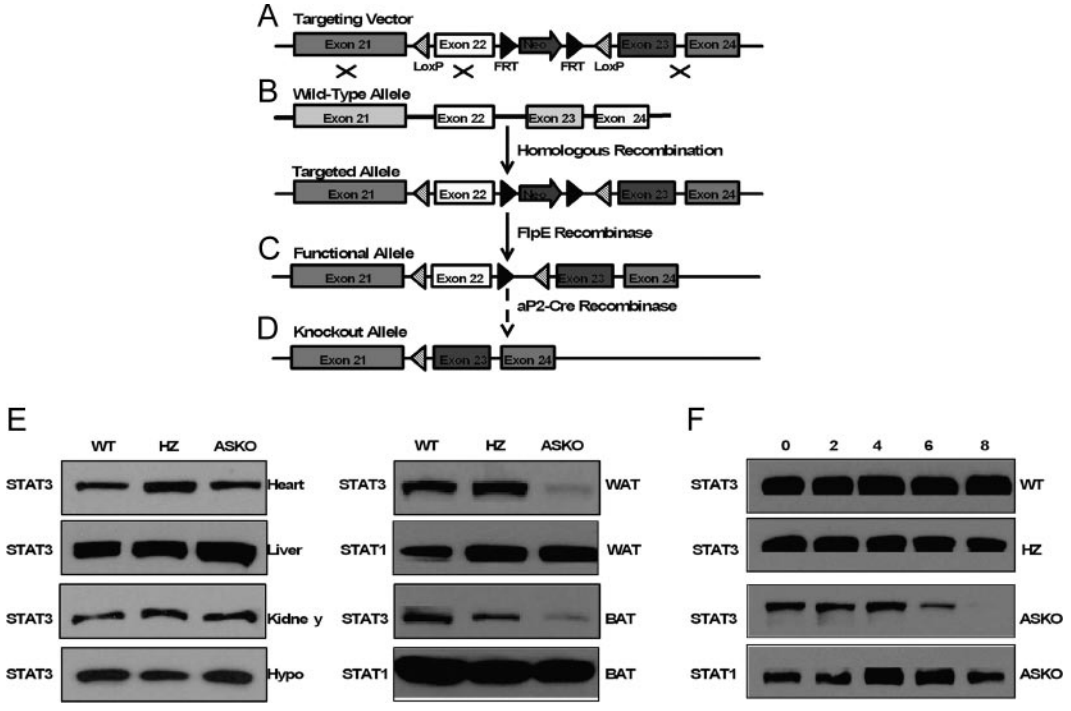

FIG. 1. Generation of ASKO mice. A–D, Schematic representation of the STAT3 targeting vector (A), the endogenous STAT3 allele before (WT allele) and after (targeted allele) homologous recombination (B), the targeted allele after FlpE recombination (functional allele) (C), and the functional allele after Cre-mediated deletion of exon 22 (knockout allele) (D); E, Western blot analysis of STAT3 protein expression in heart, liver, kidney, hypothalamus, WAT, and BAT from WT, HZ, and ASKO mice; F, Western blot analysis of STAT3 protein expression in subcutaneous primary preadipocytes isolated from WT, HZ, and ASKO mice 0, 2, 4, 6, and 8 d after induction of differentiation.

Higher body weight and increased adiposity in ASKO mice

To determine the role of adipocyte STAT3 on body weight, ASKO mice and WT and HZ littermate control mice were weighed weekly. Growth curves were normal in male and female ASKO mice from birth to 4 wk of age. Beginning at 9 wk of age, however, male ASKO mice weighed significantly more than their littermate controls (Fig. 2A). By 20 wk of age, male ASKO mice had gained 14 and 16% more weight than their WT and HZ littermates, respectively. Female growth curves, however, remained normal. To determine the basis for the higher body weight in male ASKO mice, lean mass (Fig. 2B), fat mass (Fig. 2C), and percent fat (Fig. 2D) were measured at 4, 6, 8, 12, and 16 wk by dual-energy x-ray absorptiometry. Lean mass was similar between male ASKO mice and littermate controls at all ages. Fat mass and percent fat, however, were increased in male ASKO mice beginning at 6 wk of age. These differences were statistically significant by 16 wk of age. In addition, inguinal, gonadal, retroperitoneal, and interscapular brown fat pads from male ASKO mice weighed significantly more than fat pads from littermate controls. Significant differences were observed for both absolute fat pad weight (Fig. 3B) and fat pad weight per gram body weight (Fig. 3D). Absolute liver weight was also significantly higher in male ASKO mice (Fig. 3A). Liver weight per gram body weight, however, was indistinguishable, as were absolute heart weight, heart weight per gram body weight, and absolute kidney weight. Kidney weight per gram body weight, however, was significantly lower in male ASKO mice. These results indicate that the higher body weight in male ASKO mice was due to increased adiposity.

Increased adiposity can result from an increase in adipocyte cell size (hypertrophy), an increase in adipocyte cell number (hyperplasia), or both. To determine whether adipocyte hypertrophy contributed to the increased adiposity in male ASKO mice, histological studies were carried out. Histological analysis of WAT sections from WT and ASKO mice revealed that male ASKO mice had larger adipocytes than WT mice (Fig. 3E).

To determine whether male ASKO mice displayed changes in expression levels of adipogenic transcription factors and adipocyte-specific genes, gene expression analysis of WAT from WT and ASKO mice was conducted by real-time PCR. RT-PCR revealed no differences in the expression of C/EBPα, PPARγ, and aP2 (data not shown). WAT DNA content (data not shown) was also similar between WT and ASKO mice, indicating that the increase in adipose tissue mass observed in male ASKO mice was not due to adipocyte hyperplasia.

Normal food intake and energy expenditure in ASKO mice

To determine whether the increase in adiposity in male ASKO mice was due to positive energy balance, energy intake and energy expenditure were monitored in 12-wk-old male ASKO mice and 12-wk-old WT littermate controls by an indirect calorimetry system as described in *Materials and Methods*. Analysis of food intake showed no significant differences in absolute daily food intake (Fig. 4A) or daily food intake per gram body weight (Fig. 4B). As shown in Fig. 4, C and D, horizontal activity (Xtot), ambulation (Xamb), and vertical activity (Ztot) were also similar between male ASKO

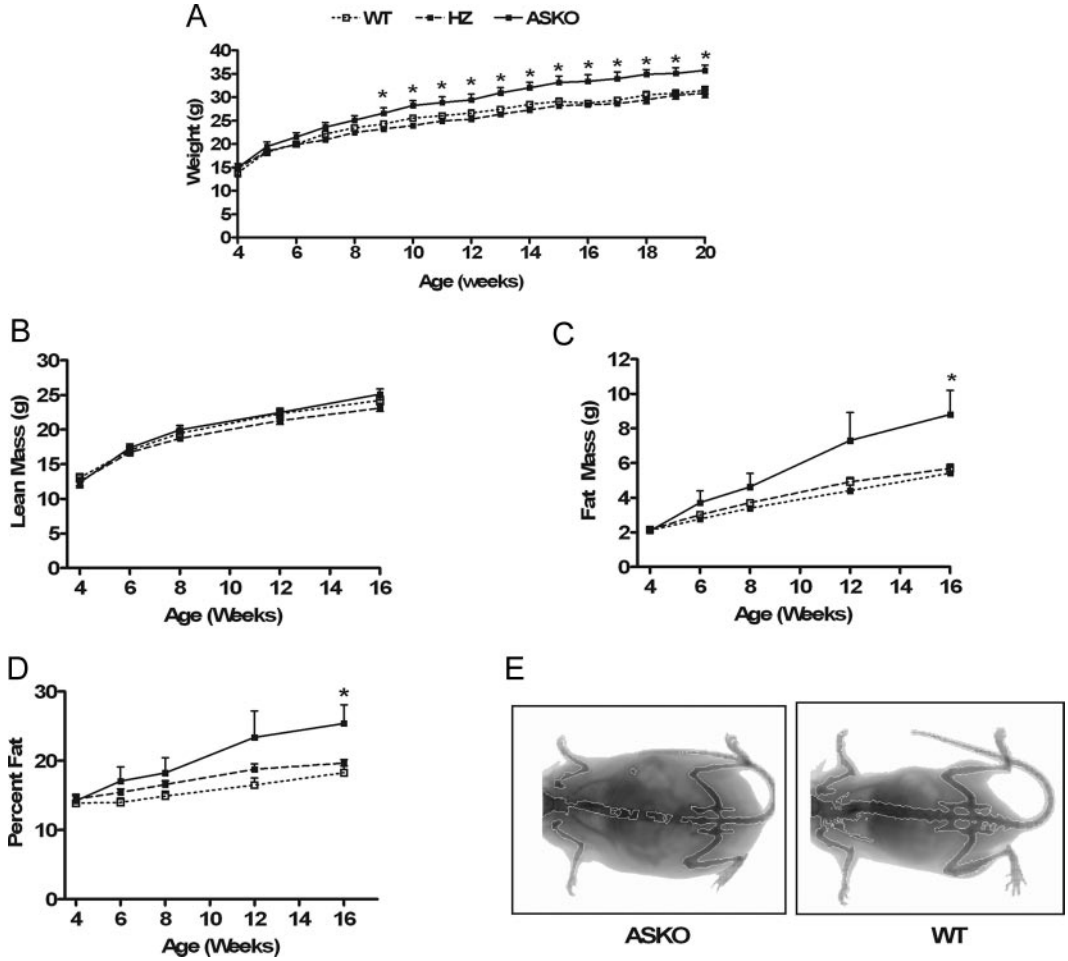

FIG. 2. Higher body weight and increased mass in ASKO mice. A, Growth curves of male ASKO mice and WT and HZ littermate controls. Data are means ± SE (n = 8–16). *, Significantly different from WT and HZ littermate controls. B–D, Lean mass (B), fat mass (C), and percent fat (D) of 4-, 6-, 8-, 12-, and 16-wk-old male ASKO mice and WT and HZ littermate controls. Data are means ± SE (n = 8–16). *, Significantly different from littermate controls. E, Representative PIXImus image of a 16-wk-old male ASKO mouse (*left*) and a 16-wk-old WT control mouse (*right*).

mice and littermate controls. Oxygen consumption normalized to body weight (Fig. 4E) and lean body mass (Fig. 4F) were also similar between male ASKO mice and littermate controls. These results indicate that the increased adiposity in male ASKO mice was not due to hyperphagia or reduced energy expenditure. The methodology employed, however, may not be sensitive enough to detect subtle long-term disturbances in energy balance. Additionally, more studies are needed to determine whether increased dietary fat absorption contributes to the higher body weight and increased adiposity.

Normal glucose tolerance in ASKO mice

To determine the metabolic consequences of loss of adipocyte STAT3, we monitored circulating glucose, insulin, leptin, TAG, and FFAs in male ASKO mice and WT littermate controls at 12–16 wk of age. Under both fed and fasting conditions, no differences were observed in blood glucose levels or serum TAG or FFA levels between male ASKO mice and WT mice (Table 1). Fasting plasma insulin and serum leptin levels were also similar between male ASKO and WT mice. Because ASKO mice and WT mice had similar blood glucose and plasma insulin concentrations, we concluded that the increased adiposity in male ASKO mice did not alter glucose homeostasis. As expected, male ASKO mice and WT mice exhibited comparable blood glucose concentrations at all time points after administration of an oral glucose load (Fig. 5A). Corresponding insulin levels (Fig. 5B) were also similar. In addition, the pancreas from male ASKO mice exhibited no gross or histological abnormalities.

Increased liver TAG in ASKO mice

Fatty liver is strongly associated with both hepatic and adipose tissue insulin resistance as well as reduced whole-body insulin sensitivity (27–29). Because male ASKO mice exhibited normal glucose tolerance, as determined by oral glucose tolerance testing, we hypothesized that the increased adiposity was limited to the adipose tissue and did not affect the liver. However, liver TAG was increased in male ASKO mice (Fig. 5C). Consistent with these data, histological analysis of liver sections from male ASKO mice also showed a marked increase in lipid deposition (Fig. 5D). Furthermore, serum adiponectin levels, which correlate negatively with

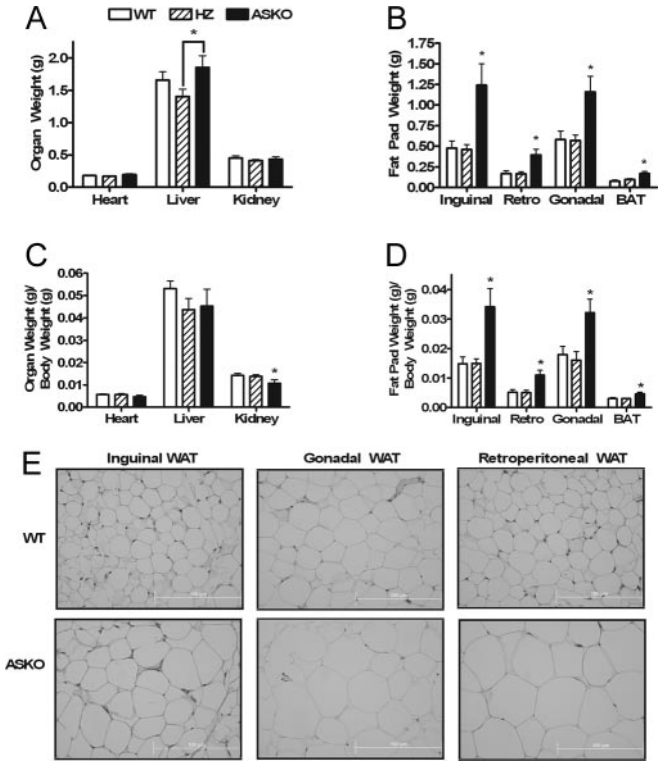

FIG. 3. Increased adiposity in ASKO mice. A–D, Absolute organ weight (A), absolute fat pad weight (B), organ weight per gram body weight (C), and fat pad weight per gram body weight (D) in 20-wk-old male ASKO mice and 20-wk-old WT and HZ littermate controls. Data are means ± SE (n = 8–12). *, Significantly different from littermate controls. E, Hematoxylin and eosin staining of inguinal WAT, gonadal WAT, and retroperitoneal WAT, from 20-wk-old male ASKO mice and 20-wk-old WT littermate controls (shown at the same magnification).

adiposity and hepatic fat (30, 31), were significantly reduced in male ASKO mice (Table 1).

Impaired leptin signaling in ASKO mice

The STAT3-activating ligand leptin induces weight loss, in part, via pro-lipolytic actions on adipose tissue (6–10, 12, 13, 32). Additionally, a leptinergic blockade, as demonstrated by a decrease in STAT3 tyrosine phosphorylation, protects diet-induced obese rodents from leptin's fat-depleting autocrine/paracrine actions (33). To determine whether loss of leptin action via disruption of STAT3 signaling was responsible for the increased adiposity in male ASKO mice, leptin-induced lipolysis studies were carried out in adipocytes differentiated in culture from preadipocytes isolated from WT and ASKO mice. Eight days after differentiation, WT and ASKO cells were stimulated with varying doses (5.0–100.0 ng/ml) of recombinant leptin (rLeptin). Glycerol released into the medium was measured after 24 h of leptin exposure. No effect was seen in either WT cells or ASKO cells stimulated with rLeptin in concentrations ranging from 5.0–50.0 ng/ml. At a concentration of 100.0 ng/ml, however, the addition of rLeptin to WT cells promoted glycerol release relative to cells treated with vehicle alone (Fig. 6A). The addition of 100.0 ng/ml rLeptin to ASKO cells, however, had no effect (Fig. 6A), suggesting that adipocyte STAT3 mediates leptin-induced lipolysis. Isoproterenol-induced lipolysis, however, was unimpaired in ASKO cells (Fig. 6A). In addition, an increase in STAT1 tyrosine phosphorylation was observed only in ASKO cells exposed to rLeptin (Fig. 6B).

Leptin also induces weight loss via anti-lipogenic actions on adipose tissue (6–10, 12, 13, 32). To determine whether loss of leptin's anti-lipogenic actions was responsible for the increased adiposity in male ASKO mice, we examined the expression of lipogenic genes. Gene expression analysis of WAT from WT and ASKO mice revealed no differences in the expression of FAS or diacylglycerol acyltransferase (DGAT) (data not shown).

Discussion

In the present studies, we show that male ASKO mice fed a standard chow diet weigh more than their littermate controls and demonstrate that the higher body weight is due to increased adiposity associated with adipocyte hypertrophy but not adipocyte hyperplasia, hyperphagia, or reduced energy expenditure. The higher body weight and increased fat mass exhibited by male ASKO mice in this study are in agreement with other tissue-specific STAT3 knockout models linking STAT3 and adiposity (34–37). Mice with a neural-specific disruption of the STAT3 gene are obese, hyperleptinemic, leptin-resistant, diabetic, and infertile. Mice with a β-cell/hypothalamic-specific disruption of the STAT3 gene are also obese, hyperphagic, hyperglycemic, and hyperinsulinemic. Additionally, inactivation of STAT3 in proopiomelanocortin neurons causes obesity as well. Unlike these models, however, a dramatic sexual dimorphism was observed in ASKO mice; only male ASKO mice became obese. Although the mechanisms causing this sex difference are unknown, they may reflect alternative pathways compensating for the lack of STAT3 in female mice. A recent study shows that aromatase-deficient mice of both sexes have a phenotype of increased adiposity (38). This obese phenotype, however, is more pronounced in female mice, suggesting that estrogen signaling pathways may have a compensatory effect on STAT3 deficiency in our female ASKO mice.

Because increased fat mass in male ASKO mice was accompanied by adipocyte hypertrophy without changes in cell number or differentiation, we concluded that increased fat mass was the result of increased TAG accumulation in preexisting adipocytes. We hypothesized that the cause of the enhanced TAG accumulation was increased fatty acid and TAG synthesis, decreased breakdown and/or export of stored TAG, or increased uptake of circulating TAG. Because the STAT3-activating ligand leptin has been shown to have both anti-lipogenic and pro-lipolytic actions in adipose tissue (6–10, 32), we speculated that loss of leptin action was responsible for the increased TAG accumulation in adipocytes from male ASKO mice. We found that leptin-induced lipolysis was impaired in adipocytes differentiated in culture from preadipocytes isolated from male ASKO mice. Isoproterenol-induced lipolysis, however, was unimpaired in ASKO cells, suggesting that leptin-induced lipolysis is dependent on STAT3, but not lipolysis induced by adrenergic stimulation. Because STAT1 was tyrosine phosphorylated in ASKO cells but not in WT cells cultured in the presence of

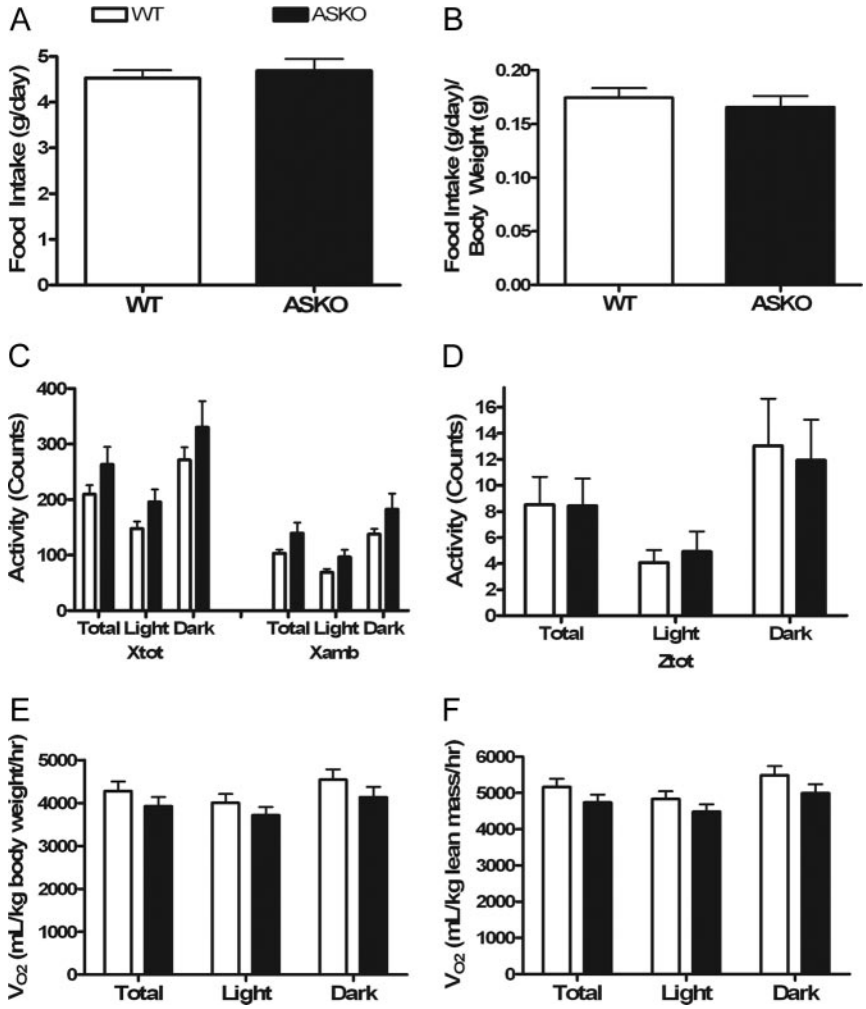

FIG. 4. Normal food intake and energy expenditure in ASKO mice. A and B, Absolute daily food intake (A) and daily food intake per gram body weight (B) in 12-wk-old male ASKO mice and 12-wk-old WT littermate controls. Data are means ± SE (n = 8–11). C and D, Horizontal activity (Xtot) and ambulation (Xamb) (C) and vertical activity (Ztot) (D) in 12-wk-old male ASKO mice and 12-wk-old WT littermate controls. Data are means ± SE (n = 8–11). E and F, VO_2 (milliliters per kilogram body weight per hour) (E) and VO_2 (milliliters per kilogram lean mass per hour) (F) in 12-wk-old male ASKO mice and 12-wk-old WT littermate controls. Data are means ± SE (n = 8–11).

rLeptin, STAT1 is likely not used as an alternative pathway in leptin-induced lipolysis. As for fatty acid and TAG synthesis, the expression of lipogenic genes was increased in WAT from male ASKO mice, but not to a significant degree. Because mRNA levels do not always correlate with enzyme activity, more studies examining the activity of lipogenic enzymes are needed to better understand the mechanism of TAG accumulation in adipocytes from ASKO mice.

Recent studies have shown a relationship between adipocyte size and adipokine expression and secretion. Serum adiponectin levels, for example, correlate inversely with adipocyte size (39, 40), whereas serum leptin levels correlate positively (41). In agreement with the significant hypertrophy of adipocytes in male ASKO mice, serum adiponectin levels were significantly reduced. Serum leptin levels, however, were not increased. There are several possible explanations for this finding. The increase in WAT TAG content may not be sufficient to trigger an increase in leptin synthesis. Furthermore, altered adipocyte differentiation is frequently associated with changes in circulating leptin levels (42–44). Response elements for adipogenic transcription factors and adipocyte-specific genes have also been identified in the leptin promoter (45). The absence of adipocyte hyperplasia in male ASKO mice, therefore, is consistent with the lack of

TABLE 1. Normal biochemical parameters in ASKO mice

	Fasted		Fed	
	WT	ASKO	WT	ASKO
Blood glucose (mg/dl)	70.44 ± 4.06	70.0 ± 4.00	123.7 ± 10.52	123.0 ± 9.08
Serum FFA (mEq/liter)	1.06 ± 0.05	1.05 ± 0.04	0.28 ± 0.04	0.26 ± 0.03
Serum TAG (mg/dl)	141.48 ± 7.14	133.96 ± 16.77	108.48 ± 3.75	108.83 ± 8.68
Plasma insulin (ng/ml)	0.82 ± 0.14	1.09 ± 0.27	ND	ND
Serum leptin (ng/ml)	1.16 ± 0.26	1.30 ± 0.46		
Serum adiponectin (μg/ml)	7.32 ± 0.28	5.48 ± 0.22[a]		

Biochemical parameters in 12–16 wk old male ASKO mice and WT littermate controls. Data are means ± SE (n = 6–10). ND, No data.
[a] Significantly different from littermate controls.

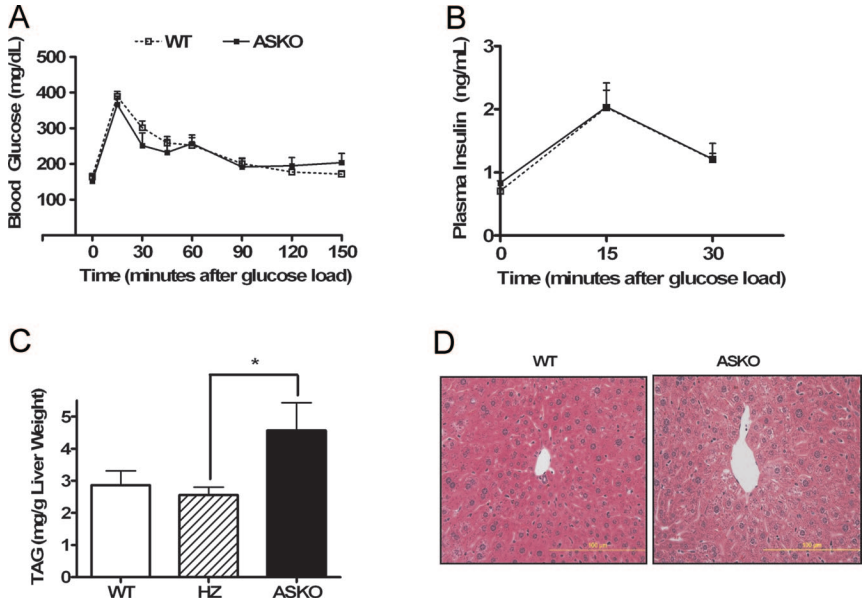

FIG. 5. Normal glucose tolerance and fatty liver in ASKO mice. A, Blood glucose concentrations during oral glucose tolerance tests in 20-wk-old male ASKO mice and WT littermate controls. Data are means ± SE (n = 8–11). B, Plasma insulin concentrations during oral glucose tolerance tests in 20-wk-old male ASKO mice and WT and HZ littermate controls. Data are means ± SE (n = 6). C, Liver TAG content in 20-wk-old male ASKO mice and WT and HZ littermate controls. Data are means ± SE (n = 4–6). *, Significantly different from littermate controls. D, Hematoxylin and eosin staining of liver sections from 20-wk-old male ASKO mice and 20-wk-old WT littermate controls (shown at the same magnification).

increased serum leptin levels. Additionally, it has been shown that circulating FFAs stimulate leptin secretion (32, 46). Thus, the absence of increased serum FFAs in male ASKO mice is also consistent with the observed normal circulating leptin levels.

Because male ASKO mice developed a fatty liver, however, it is notable that they did not exhibit elevated FFAs. The fact that serum fatty acids were not increased in these animals suggests that an increased supply of fatty acids to the liver is not the cause of the steatosis. Rather, an imbalance in liver TAG synthesis, export, or oxidation is likely the cause. It has been shown that high adiponectin levels protect against fatty liver by reducing fatty acid synthesis through inhibition of acetyl-coenzyme A (CoA) carboxylase (ACC) and FAS expression and activity (47). The reduction of acetyl-CoA carboxylase activity also reduces the malonyl CoA level, which is known to inhibit carnitine palmitoyltransferase I (CPT-1) activity and fatty acid oxidation. Therefore, we speculate that the reduced serum adiponectin levels in male ASKO mice likely increase fatty acid synthesis and reduce fatty acid oxidation, thus causing the fatty liver. Additional studies examining changes in gene expression and enzyme activity are needed to understand the exact cause of the TAG accumulation in the livers of male ASKO mice.

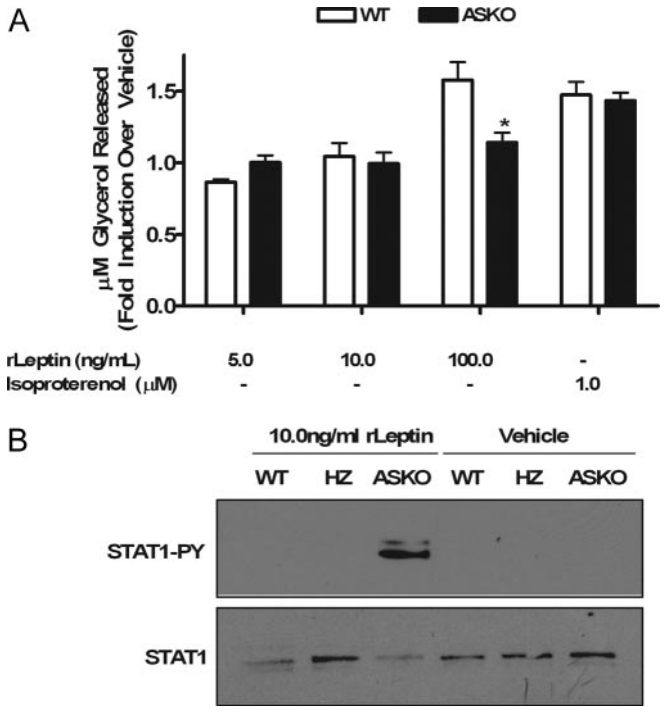

FIG. 6. Impaired leptin signaling in ASKO mice. A, Glycerol released from WT and ASKO cells stimulated with varying doses of rLeptin or isoproterenol. Data are means ± SE from triplicate dishes repeated three times. B, Western blot analysis of STAT1 tyrosine phosphorylation in sc primary preadipocytes isolated from WT and ASKO mice cultured in the presence of 10.0 ng/ml rLeptin for 24 h.

It is also notable that whereas male ASKO mice are obese and develop adipocyte hypertrophy and a fatty liver, they exhibit normal glucose tolerance on a standard chow diet. The ASKO mouse model is not the only mouse model in which obesity is dissociated from impaired glucose tolerance. Mice lacking AMP-activated protein kinase-α2 (AMPKα2) exhibit increased adiposity and adipocyte hypertrophy but show no differences in glucose tolerance or insulin sensitivity compared with WT mice (48). Mice that overexpress phosphoenolpyruvate carboxykinase (PEPCK) in WAT also have increased adipose tissue mass but do not develop insulin resistance (49). Similarly, mice that overexpress DGAT-1 in WAT have larger adipocytes and greater total fat pad weight. The increased adiposity, however, is not associated with impaired glucose disposal (50). Finally, obesity is dissociated from insulin resistance in aP2-deficient mice fed a high-fat diet (51). We cannot rule out the possibility, however, that the obesity, adipocyte hypertrophy, and fatty liver are not sufficient to trigger insulin resistance. It is possible that with age or after a long-term challenge with a high-fat diet, male ASKO mice may develop insulin resistance. Furthermore, because fat accumulation in the liver is

a primary event leading to insulin resistance (52–54), it is also possible that as the severity of the fatty liver worsens, ASKO mice may develop insulin resistance as well.

In summary, here we show that loss of STAT3 in mature adipocytes in male mice causes higher body weight, increased adiposity associated with adipocyte hypertrophy, reduced serum adiponectin levels, and fatty liver but not impaired glucose tolerance. We also show that loss of leptin action in WAT, namely loss of leptin-induced lipolysis, may play a role in the observed obese phenotype. The results of our study clearly demonstrate that STAT3 is essential for body weight homeostasis, although more studies are needed to better clarify its role in this regard, especially as it relates to the development of obesity in ASKO mice.

Acknowledgments

We thank Randy J. Thresher and Kimberly D. Kluckman for assistance with creation of knockout mice and Feng Li, Patricia A. Sheridan, Alexia G. Smith, and Nobuyuki Takahashi for assistance with real-time PCR.

Received August 20, 2007. Accepted December 12, 2007.

Address all correspondence and requests for reprints to: Joyce B. Harp, M.D., Department of Nutrition, CB 7461 McGavran Greenberg Hall, University of North Carolina at Chapel Hill, Chapel Hill, North Carolina 27599. E-mail: jharp@email.unc.edu.

This work was supported by the U.S. Public Health Service Grants DK-53398 and DK-59337 from the National Institute of Diabetes and Digestive and Kidney Diseases (NIDDK). This work was supported in part by the National Institutes of Health (NIH)/NIDDK Nutrition Training Grant DK-07686 (to E.R.C.), and by NIH Grants DK56350 (University of North Carolina Clinical Nutrition Research Unit) and DK-34987 (University of North Carolina Cell Service and Histology Core).

Disclosure Statement: E.R.C, J.D, M.C.B, and T.P.C. have nothing to declare. J.B.H. is currently employed by and has equity interest in Merck & Co.

References

1. **Popkin B, Doak C** 1998 The obesity epidemic is a worldwide phenomenon. Nutr Rev 56:106–114
2. **Hausman D, Digirolamo M, Bartness T, Hausman G, Martin R** 2001 The biology of white adipocyte proliferation. Obes Rev 2:239–254
3. **Rosen E, MacDougald O** 2006 Adipocyte differentiation from the inside out. Nat Rev Mol Cell Biol 7:885–896
4. **Stephens JM, Morrison RF, Pilch PF** 1996 The expression and regulation of STATs during 3T3-L1 adipocyte differentiation. J Biol Chem 271:10441–10444
5. **Deng J, Hua K, Lesser SS, Harp JB** 2000 Activation of signal transducer and activator of transcription-3 during proliferative phases of 3T3–L1 adipogenesis. Endocrinology 141:2370–2376
6. **Siegrist-Kaiser CA, Pauli V, Juge-Aubry CE Boss O, Pernina, Chin WW, Cusin I, Rohner-Heanrenaud F, Burger AG, Zapf J, Meier CA** 1997 Direct effects of leptin on brown and white adipose tissue. J Clin Invest 100:2858–2864
7. **Chen G, Koyama K, Yuan X, Lee Y, Zhou YT, O'Doherty R, Newgard CB, Unger RH** 1996 Disappearance of body fat in normal rats induced by adenovirus-mediated leptin gene therapy. Proc Natl Acad Sci USA 93:14795–14799
8. **Shimabukuro M, Koyama K, Chen G, Wang MY, Trieu F, Lee Y, Newgard CB, Unger RH** 1997 Direct anti-diabetic effect of leptin through triglyceride depletion of tissues. Proc Natl Acad Sci USA 94:4637–4641
9. **Fruhbeck G, Aguado M, Martinez JA** 1997 In vitro lipolytic effect of leptin on mouse adipocytes: evidence for a possible autocrine/paracrine role of leptin. Biochem Biophys Res Commun 240:590–594
10. **Fruhbeck G, Aguado M, Gomez-Ambrosi J, Martinez JA** 1998 Lipolytic effect of in vivo leptin administration on adipocytes of lean and Ob/Ob mice, but not dB/dB mice. Biochem Biophys Res Commun 250:99–102
11. **Wang M-Y, Lee Y, Unger RH** 1999 Novel form of lipolysis induced by leptin. J Biol Chem 274:17541–17544
12. **Bai Y, Zhang S, Kim KS, Lee JK, Kim KH** 1996 Obese gene expression alters the ability of 30A5 preadipocytes to respond to lipogenic hormones. J Biol Chem 271:13939–13942
13. **Zhou Y, Wang Z, Higa M, Newgard C, Unger R** 1999 Reversing adipocyte differentiation: implications for treatment of obesity. Proc Natl Acad Sci USA 96:2391–2395
14. **Path G, Bornstein SR, Gurniak M, Chrousos GP, Scherbaum WA, Hauner H** 2001 Human breast adipocytes express interleukin-6 (IL-6) and its receptor system: increased IL-6 production by β-adrenergic activation and effects of IL-6 on adipocyte function. J Clin Endocrinol Metab 86:2281–2288
15. **Trujillo ME, Sullivan S, Harten I, Schneider SH, Greenberg AS, Fried SK** 2004 Interleukin-6 regulates human adipose tissue lipid metabolism and leptin production *in vitro*. J Clin Endocrinol Metab 89:5577–5582
16. **Greenberg A, Nordan R, Mcintosh J, Calvo J, Scow R, Jablons D** 1992 Interleukin 6 reduces lipoprotein lipase activity in adipose tissue of mice in vivo and in 3T3-L1 adipocytes: a possible role for interleukin 6 in cancer cachexia. Cancer Res 52:4113–4116
17. **Van Hall G, Steensberg A, Sacchetti M, Fischer C, Keller C, Schjerling P, Hiscock N, Moller K, Saltin B, Febbraio MA, Pedersen BK** 2003 Interleukin-6 stimulates lipolysis and fat oxidation in humans. J Clin Endocrinol Metab 88:3005–3010
18. **Lyngso D, Simonsen L, Bulow J** 2002 Metabolic effects of interleukin-6 in human splanchnic and adipose tissue. J Physiol (Lond) 543:379–386
19. **Zvonic S, Cornelius P, Stewart WC, Mynatt RL, Stephens JM** 2003 The regulation and activation of ciliary neurotrophic factor signaling proteins in adipocytes. J Biol Chem 278:2228–2235
20. **Sleeman M, Anderson K, Lambert P, Yancopoulos G, Wiegand S** 2000 The ciliary neurotrophic factor and its receptor, CNTFα. Pharm Acta Helv 74:265–272
21. **Rodbell M** 1964 Metabolism of isolated fat cells. I. Effects of hormones on glucose metabolism and lipolysis. J Biol Chem 239:375–380
22. **Folch J, Lees M, Stanley GHS** 1957 A simple method for the isolation and purification of total lipids from animal tissues. J Biol Chem 226:497–509
23. **Zhong Z, Wen Z, Darnell JJ** 1994 Stat3: a STAT family member activated by tyrosine phosphorylation in response to epidermal growth factor and interleukin-6. Science 264:95–98
24. **Tontonoz P, Hu E, Graves R, Budavari A, Spiegelman B** 1994 mPPARγ2: tissue-specific regulator of an adipocyte enhancer. Genes Dev 8:1224–1234
25. **Soukas A, Socci ND, Saatkamp BD, Novelli S, Friedman JM** 2001 Distinct transcriptional profiles of adipogenesis in vivo and in vitro. J Biol Chem 276:34167–34174
26. **Tchoukalova YD, Sarr MG, Jensen MD** 2004 Measuring committed preadipocytes in human adipose tissue from severely obese patients by using adipocyte fatty acid binding protein. Am J Physiol Regul Integr Comp Physiol 287:R1132–R1140
27. **Marchesini G, Brizi M, Bianchi G, Tomassetti S, Bugianesi E, Lenzi M, Mccullough AJ, Natale S, Forlani G, Melchionda N** 2001 Nonalcoholic fatty liver disease: a feature of the metabolic syndrome. Diabetes 50:1844–1850
28. **Bugianesi E, Gastaldelli A, Vanni E, Gambino R, Cassader M, Baldi S, Ponti V, Pagano G, Ferrannini E, Rizzetto M** 2005 Insulin resistance in non-diabetic patients with non-alcoholic fatty liver disease: sites and mechanisms. Diabetologia 48:634–642
29. **Seppala-Lindroos A, Vehkavaara S, Hakkinen A-M, Goto T, Westerbacka J, Sovijarvi A, Halavaara J, Yki-Jarvinen H** 2002 Fat accumulation in the liver is associated with defects in insulin suppression of glucose production and serum free fatty acids independent of obesity in normal men. J Clin Endocrinol Metab 87:3023–3028
30. **Bugianesi E, Pagotto U, Manini R, Vanni E, Gastaldelli A, De Lasio R, Gentilcore E, Natale S, Cassader M, Rizzetto M, Pasquali R, Marchesini G** 2005 Plasma adiponectin in nonalcoholic fatty liver is related to hepatic insulin resistance and hepatic fat content, not to liver disease severity. J Clin Endocrinol Metab 90:3498–3504
31. **Hui J, Hodge A, Farrell G, Kench J, Kriketos A, George J** 2004 Beyond insulin resistance in NASH: TNF-α or adiponectin? Hepatology 40:46–54
32. **Wang J, Liu R, Hawkins M, Barzilai N, Rossetti L** 1998 A nutrient-sensing pathway regulates leptin gene expression in muscle and fat. Nature 393:684–688
33. **Wang M-Y, Orci L, Ravazzola M, Unger RH** 2005 Fat storage in adipocytes requires inactivation of leptin's paracrine activity: implications for treatment of human obesity. Proc Natl Acad Sci USA 102:18011–18016
34. **Gao Q, Wolfgang MJ, Neschen S, Morino K, Horvath TL, Shulman GI, Fu XY** 2004 Disruption of neural signal transducer and activator of transcription 3 causes obesity, diabetes, infertility, and thermal dysregulation. Proc Natl Acad Sci USA 101:4661–4666
35. **Cui Y, Huang L, Elefteriou F, Yang G, Shelton JM, Giles JE, Oz OK, Pourbahrami T, Lu CY, Richardson JA, Karsenty G, Li C** 2004 Essential role of STAT3 in body weight and glucose homeostasis. Mol Cell Biol 24:258–269
36. **Inoue H, Ogawa W, Ozaki M, Haga S, Matsumoto M, Furukawa K, Hashimoto N, Kido Y, Mori T, Sakaue H, Teshigawara K, Jin S, Iguchi H, Hiramatsu R, Leroith D, Takeda K, Akira S, Kasuga M** 2004 Role of STAT-3 in regulation of hepatic gluconeogenic genes and carbohydrate metabolism in vivo. Nat Med10:168–174
37. **Xu Aw, Ste-Marie L, Kaelin CB, Barsh GS** 2007 Inactivation of signal transducer and activator of transcription 3 in proopiomelanocortin (POMC) neurons causes decreased POMC expression, mild obesity, and defects in compensatory refeeding. Endocrinology 148:72–80
38. **Jones M, Thorburn A, Britt KL, Hewitt KN, Wreford NG, Proietto J, Oz OK, Leury BJ, Robertson KM, Yao S, Simpson ER** 2000 Aromatase-deficient

(ARKO) mice have a phenotype of increased adiposity. Proc Natl Acad Sci USA 97:2735–2740
39. **Arita Y, Kihara S, Ouchi N, Takahashi M, Maeda K, Miyagawa J, Hotta K, Shimomura I, Nakamura T, Miyaoka K, Kuriyama H, Nishida M, Yamashita S, Okubo K, Matsubara K, Muraguchi M, Ohmoto Y, Funahashi T, Matsuzawa Y** 1999 Paradoxical decrease of an adipose-specific protein, adiponectin, in obesity. Biochem Biophys Res Commun 257:79–83
40. **Hu E, Liang P, Spiegelman BM** 1996 AdipoQ is a novel adipose-specific gene dysregulated in obesity. J Biol Chem 271:10697–10703
41. **Friedman JM, Halaas JL** 1998 Leptin and the regulation of body weight in mammals. Nature 395:763–770
42. **Lin J, Arnold HB, Della-Fera MA, Azain MJ, Hartzell DL, Baile CA** 2002 Myostatin knockout in mice increases myogenesis and decreases adipogenesis. Biochem Biophys Res Commun 291:701–706
43. **He W, Barak Y, Hevener A, Olson P, Liao D, Le J, Nelson M, Ong E, Olefsky JM, Evans RM** 2003 Adipose-specific peroxisome proliferator-activated receptor γ knockout causes insulin resistance in fat and liver but not in muscle. Proc Natl Acad Sci USA 100:15712–15717
44. **Lee K, Villena J, Moon Y, Kim KH, Lee S, Kang C, Sul HS** 2003 Inhibition of adipogenesis and development of glucose intolerance by soluble preadipocyte factor-1 (Pref-1). J Clin Invest 111:453–461
45. **Gong DW, Bi S, Pratley RE, Weintraub BD** 1996 Genomic structure and promoter analysis of the human obese gene. J Biol Chem 271:3971–3974
46. **Fabris R, Nisoli E, Lombardi AM, Tonello C, Serra R, Granzotto M, Cusin I, Rohner-Jeanrenaud F, Federspil G, Carruba MO Vettor R** 2001 Preferential channeling of energy fuels toward fat rather than muscle during high free fatty acid availability in rats. Diabetes 50:601–608
47. **Xu A, Wang Y, Keshaw H, Xu L, Lam K, Cooper G** 2003 The fat-derived hormone adiponectin alleviates alcoholic and nonalcoholic fatty liver diseases in mice. J Clin Invest 112:91–100
48. **Villena JA, Viollet B, Andreelli F, Kahn A, Vaulont S, Sul HS** 2004 Induced adiposity and adipocyte hypertrophy in mice lacking the AMP-activated protein kinase-α2 subunit. Diabetes 53:2242–2249
49. **Franckhauser S, Munoz S, Pujol A, Casellas A, Riu E, Otaegui P, Su B, Bosch F** 2002 Increased fatty acid re-esterification by PEPCK overexpression in adipose tissue leads to obesity without insulin resistance Diabetes 51:624–630
50. **Chen HC, Stone SJ, Zhou P, Buhman KK, Farese Jr RV** 2002 Dissociation of obesity and impaired glucose disposal in mice overexpressing acyl coenzyme A:diacylglycerol acyltransferase 1 in white adipose tissue. Diabetes 51:3189–3195
51. **Hotamisligil G, Johnson R, Distel R, Ellis R, Papaioannou V, Spiegelman B** 1996 Uncoupling of obesity from insulin resistance through a targeted mutation in aP2, the adipocyte fatty acid binding protein. Science 274:1377–1379
52. **Dresner A, Laurent D, Marcucci M, Griffin ME, Dufour S, Cline GW, Slezak LA, Andersen DK, Hundal RS, Rothman DL, Petersen KF, Shulman GI** 1999 Effects of free fatty acids on glucose transport and IRS-1-associated phosphatidylinositol 3-kinase activity. J Clin Invest 103:253–259
53. **Griffin M, Marcucci M, Cline G, Bell K, Barucci N, Lee D, Goodyear LJ, Kraegen EW, White MF, Shulman GI** 1999 Free fatty acid-induced insulin resistance is associated with activation of protein kinase Cθ and alterations in the insulin signaling cascade. Diabetes 48:1270–1274
54. **Randle P, Garland P, Hales C, Newsholme E** 1963 The glucose fatty-acid cycle: its role in insulin sensitivity and the metabolic disturbances of diabetes mellitus. Lancet 1:785–789

***Endocrinology* is published monthly by The Endocrine Society (http://www.endo-society.org), the foremost professional society serving the endocrine community.**